ELSEVIER

Materials Science and Engineering A 474 (2008) 30–38

MATERIALS SCIENCE & ENGINEERING A

www.elsevier.com/locate/msea

Effect of thermal treatment on the fatigue crack propagation behavior of a new Ni-base superalloy

Xingbo Liu [a,*], Jing Xu [a], Ever Barbero [a], Wei-Di Cao [b], Richard L. Kennedy [b]

[a] *West Virginia University, Morgantown, WV 26506-6106, USA*

[b] *Allvac, an ATI Technologies Company, Monroe, NC 28111-5030, USA*

Received 22 October 2006; received in revised form 23 March 2007; accepted 10 May 2007

Abstract

The effect of various thermal treatments, including direct aging, pre-treatment, and long-term exposure, on the hold-time fatigue crack propagation behavior of 718Plus alloy were investigated and the results are summarized as follows: (1) The hold-time fatigue crack propagation rates (FCPRs) of the direct aged (DA) sample is almost the same as that of the 718Plus alloy after conventional solution plus age heat treatment. The FCP of the DA sample is slower than the conventional 718Plus alloy at 650 °C, under 3S loading condition; (2) the long-term exposure tests show that the alloy's hold-time fatigue crack resistance is improved after being exposed at 760 °C for 350 h; (3) the fine-grain alloy shows better hold-time FCP resistance than coarse-grain alloy, which is attributed to the δ-phase effect; and (4) after pre-treatment at 857 °C for up to 24 h, the alloy's fatigue crack resistance is improved because of the δ-phase at the grain boundaries.

Keywords: 718Plus; Fatigue crack propagation; Thermal treatment; δ-Phase

1. Introduction

1.1. Fatigue crack propagation (FCP) of superalloys

FCP behavior of high temperature alloys has received a great deal of attention [1]. It has been confirmed that there are a lot of parameters, which are responsible for the crack growth [2]. These parameters can be divided into three categories: (1) mechanical parameters, which include loading stresses, frequency, loading waveform, etc.; (2) material factors, which include alloy chemistry, heat treatment, and microstructure and so on; and (3) environmental factors, which include test temperature and gas environment. It should be noted that the influence of these parameters on the deformation mechanisms and failure processes in high temperature materials depends on a complex interaction amongst the parameters.

FCP of superalloys at room and at relatively lower temperatures are cycle dependent. Testing parameters, such as cycle period and waveform, play a negligible role in determining how fast the crack will grow for a fixed Δk. However, as the temperature increases beyond 500 °C, superalloys start to show a time-dependent component of FCP. The role of the environment in the fatigue behavior of superalloys has to be taken into account when the life prediction of the component is calculated. In general, the time-dependency of FCP has been attributed to two reasons: creep and environmental damage.

1.2. Microstructural effect on hold-time FCP

Time-dependent FCP is greatly affected by the microstructure of the alloys. Since both creep and environmental damage are related to grain boundary behaviors, increasing the grain size can generally improve the resistance of the alloys to time-dependent FCP by reducing the total surface area of the grain boundaries. Regarding strengthening precipitates, decreasing the γ' size from 100 to 10 nm in Waspaloy is observed to increase the FCP resistance by an approximate factor of 3 [3]. Besides the strengthening phases, gamma-prime and gamma-double prime, other grain boundary phases can play a significant role in LCF and hold-time FCP of superalloys. For instance, several detrimental phases such as the G-phase, σ-phase, and the Laves phase, can embrittle the superalloys; on the other hand, the grain boundary δ-phase has been shown to improve the FCP of the Inconel 718 alloy [4]. Investigations on Inconel 783 alloy

* Corresponding author. Tel.: +1 304 2933111x2324; fax: +1 304 2936689.
E-mail address: xingbo.liu@mail.wvu.edu (X. Liu).

0921-5093/$ – see front matter © 2007 Elsevier B.V. All rights reserved.
doi:10.1016/j.msea.2007.05.033

Table 1
Chemical composition (wt%) of Allvac 718Plus in comparison with alloy 718 and Waspaloy

Alloy	C	Ni	Cr	Mo	W	Co	Fe	Nb	Ti	Al
718Plus	0.020	Balance	18	3.0	1.0	9.0	10	5.4	0.7	1.4
718	0.025	Balance	18	3.0	–	–	18	5.4	1.0	0.5
Waspaloy	0.035	Balance	19.5	4.2	–	13.0	–	–	3.0	1.3

showed that the grain boundary β-phase improves hold-time FCP resistance of the alloy by improving the alloys' SAGBO resistance, helps in deflecting crack path, and oxide-induced crack closure [5,6].

1.3. 718Plus alloy

In recent years, a new Ni-base superalloy, Allvac 718Plus, has been developed to meet the objective of increasing the temperature capability by 55 °C as compared to alloy 718, and with comparable processing characteristics [7]. The nominal chemical composition of the alloy is listed in Table 1, as compared with that of alloy 718 and Waspaloy.

Studies demonstrated that this alloy has shown superior tensile and stress rupture properties as compared to alloy 718 and comparable properties to Waspaloy at temperatures up to 704 °C [8,9]. However, relatively speaking, the data on fatigue crack propagation (FCP) resistance of this alloy is still insufficient. FCPRs of the 718Plus alloy at conventional solution plus age condition was previously evaluated for a test frequency of 0.33 Hz with 100 s hold at maximum load, as compared to that of alloy 718 and Waspaloy [10]. Fig. 1(a) shows that alloys 718Plus, 718 and Waspaloy have similar fatigue crack growth rates under 3 s triangle loading at 650 °C with 718Plus being slightly better. As indicated in Fig. 1(b), Waspaloy shows the best resistance to fatigue crack growth under hold-time fatigue condition while the resistance of 718Plus is better than that of alloy 718.

The objective of this paper is to investigate the effect of various thermal treatments, including direct aging, pre-solution treatment, and long-term exposure, on the hold-time fatigue crack propagation behavior of the 718Plus alloy.

Table 2
Tested samples

Heat treatment	CH		CH + LE		DA	PST + CH
Grain size	8–10	4–6	8–10	4–6	8–10	4–6
Sample no.	A1	B1	A2	B2	A3	B3

Note: CH, conventional heat treatment: 955 °C/1 h/AC + 787 °C/2 h/FC → 650 °C/8 h/AC; LE, long-term exposure: 760 °C/350 h; DA, direct aging after forging; PST, pre-solution treatment: 857 °C/24 h to precipitate δ-phase before CH.

2. Experiments

2.1. Materials

The 718Plus alloy employed in this investigation was provided by ATI Allvac (Monroe, NC). The alloys were melted by vacuum induction melting plus vacuum arc remelting (1.5 tonnes) and forged to a 200 mm round billet after, which it was subjected to various thermal treatments. The samples used in this study are summarized in Table 2.

2.2. Fatigue crack propagation test

FCP tests were performed by employing the single-edge-notched (SEN) specimens, see Fig. 2. The specimens were pre-cracked up to 2.54 mm with lower stress intensity triangle cycles at room temperature. They were then heated to a higher temperature for the fatigue crack growth tests. The tests were carried out at high temperatures and with different loading cycles (3 s triangle wave, trapezoid wave with 3 + 100 s loading at maximum stress). The tests were conducted under load control. The stress intensity ratio (K_{min}/K_{max}) was always set to 0.1. Frac-

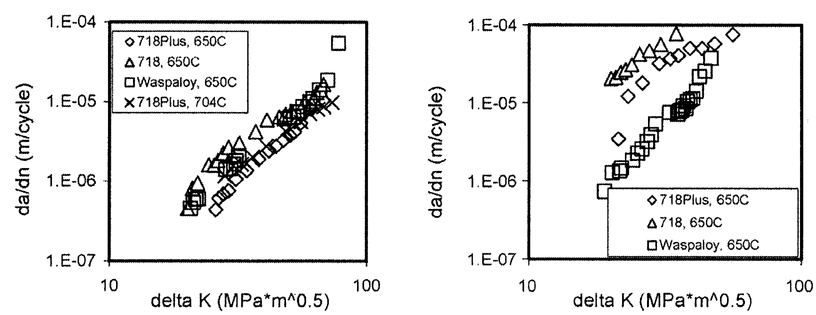

(a) 3S –triangle (b) 3+100S – trapezoid

Fig. 1. Fatigue crack propagation behaviors of 718PLUS^{TM} alloy at 650 °C, as compared to that of alloy 718 and Waspaloy.

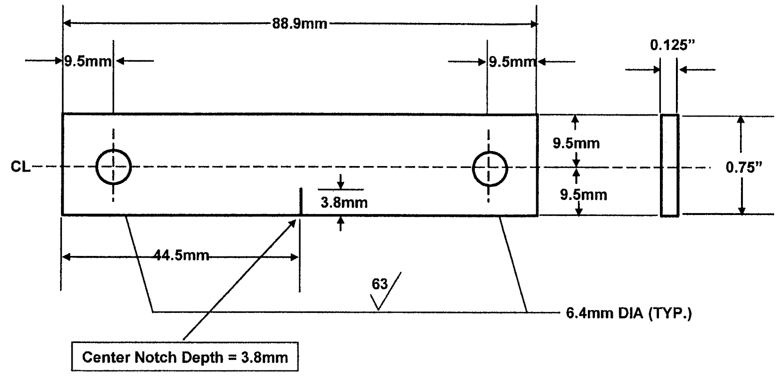

Fig. 2. Dimensions of the single-edge-notched specimens.

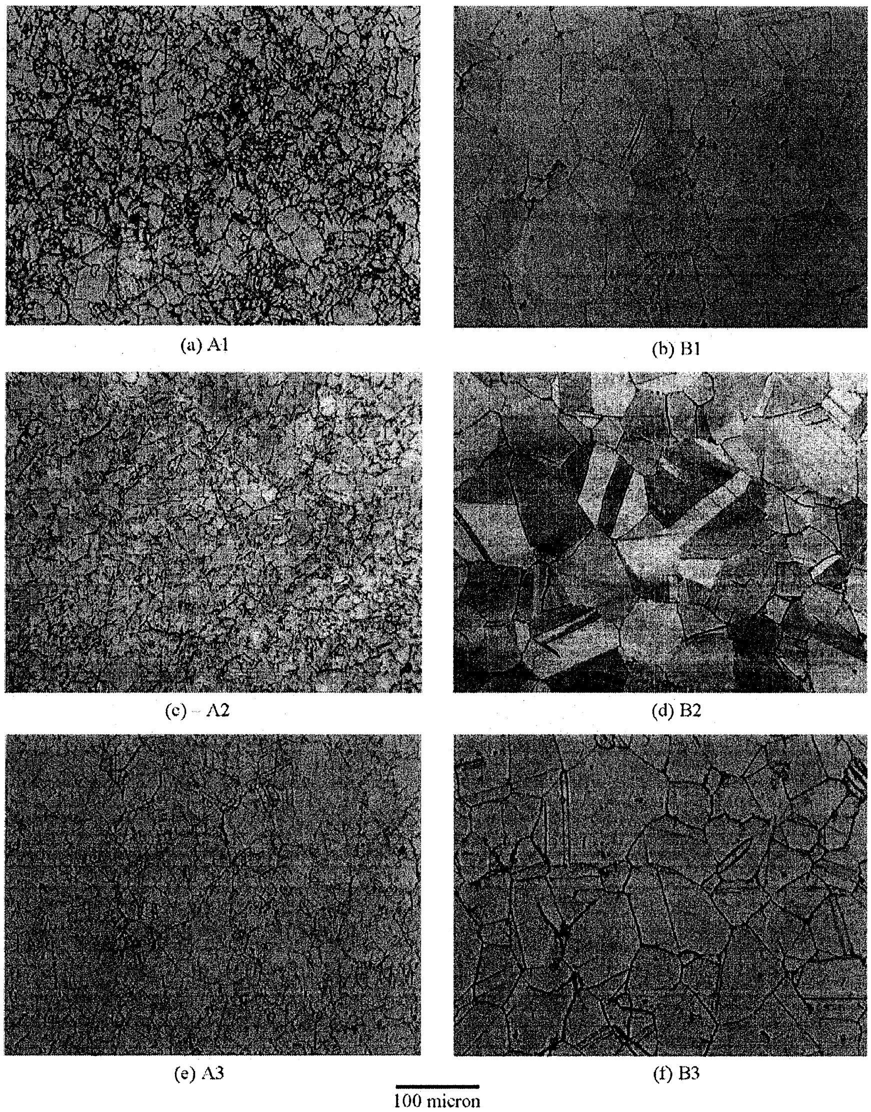

Fig. 3. Grain structure of tested samples.

tographical analyses were conducted by means of a scanning electronic microscope (SEM).

The increment in the crack length during fatigue and sustained crack growth tests was monitored continuously by a dc potential drop technique. While a constant dc current was passed through the specimen, the crack length was monitored by a pair of potential probes mounted on the front edge of the specimen across the pre-machined notch. The measured dc potential drop at any crack length was normalized and converted into the corresponding crack length by a single analytical relation, called the Johnson's equation given:

$$A = \frac{2W}{\pi} \times \cos^{-1} \times \left[\frac{\cosh(\pi Y/2W)}{\cosh\{(U/U_0)\cosh^{-1}[\cosh(\pi Y/2W)/\cos \pi A_0/2W]\}}\right] \quad (1)$$

where A and A_0 represent the actual and initial crack lengths, respectively, U and U_0 are updated and initial measured potential drops, respectively, and W, Y represent the specimen width and one half of the potential probe span, respectively.

Many different mathematical expressions for the stress intensity of a SEN specimen are available, and we use Tada's empirical equation for its accuracy over a wide range of crack lengths.

$$K = \frac{P}{\sqrt{W}} \frac{\sqrt{2\tan\theta}}{\cos\theta} \left[0.752 + 2.02\left(\frac{A}{W}\right) + 0.37(1 - \sin\theta)^3\right] \quad (2)$$

where P represents the applied load, θ equals to $(\pi/2) \times (Y/W)$. W, Y and A have the same meaning as in Eq. (1). The accuracy of this equation has been confirmed to be better than 0.5% provided that no bending moment is applied.

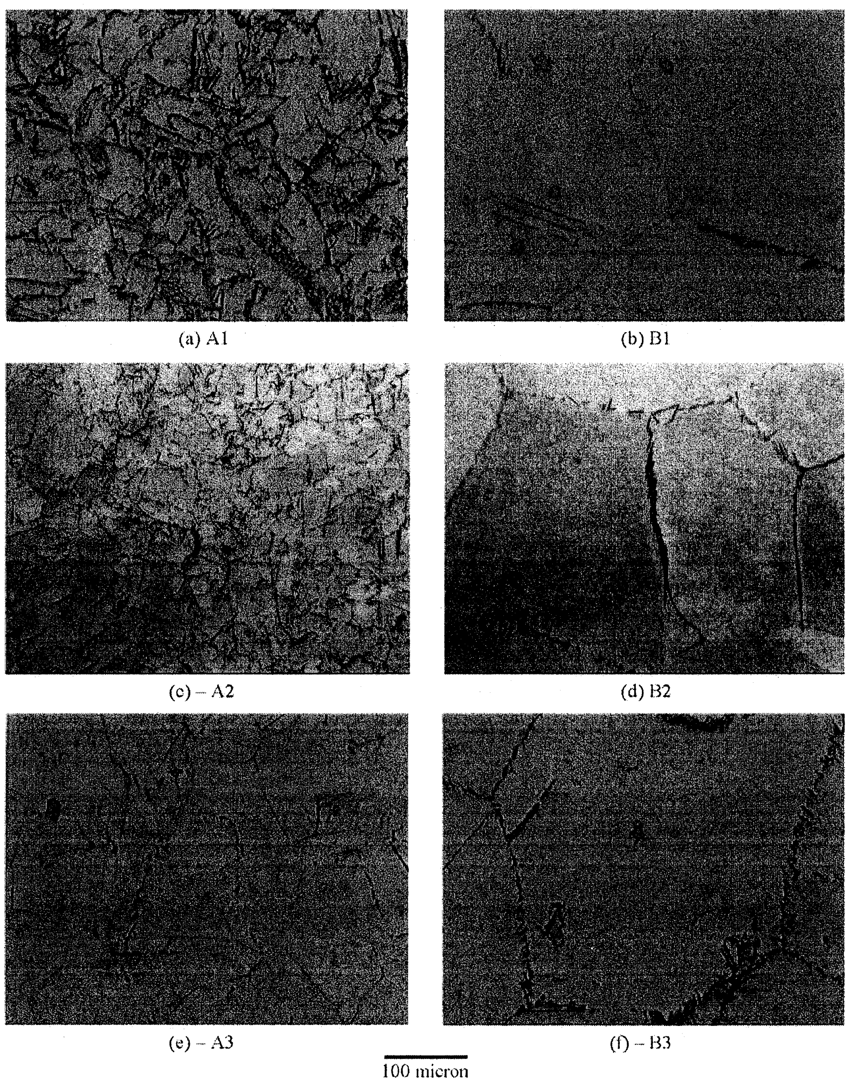

Fig. 4. Grain boundary δ-phase distribution of tested samples.

3. Experimental results

3.1. Microstructure of the material

The grain sizes of the tested samples are shown in Fig. 3, and Fig. 4 shows δ-phase morphology along with the grain boundaries of these samples. It is found from these pictures that (1) the grain sizes for A1 and B1 are ASTM 8–10 and 4–6, respectively; (2) there is more grain boundary δ-phase in A1 than B1; (3) the 760 °C/350 h exposure (A2 and B2) does not significantly change the grain size and grain boundary δ-phase morphology of A1 and B1; (3) the DA sample shows slightly elongated grain structure; and (4) pre-solution treatment (B3) increases the amount of grain boundary δ-phase, as compared to the original B1 sample.

3.2. FCP of 718Plus with various grain sizes

FCPRs of the 718Plus alloy with various grain sizes were evaluated with a test frequency of 0.33 Hz and with 100 s hold at maximum load. It is indicated by Fig. 5 that the FCPRs of groups B1 and A1 are almost the same, while FCPRs of B1 are slightly lower than that of group A1 for the tests without hold-time at 650 and 704 °C. It is also shown in Fig. 3 that contrary to the results of the tests without hold-time, the tests with 100 s hold-time revealed that the FCPs of the fine-grained A1 are slower than that of B1 at 650 °C.

As shown in Fig. 6(a), examination of the fatigue fracture surface by SEM revealed transgranular crack propagation with striations for group A1 at room temperature. The fracture mode of A1 at 650 °C is a combination of intergranular and transgranular modes. When the temperature is increased to 704 °C, the intergranular mode is predominant and the whole surface is covered by a layer of oxide film, indicating that extensive oxidation happens during the crack growth. Fig. 7 shows the fracture surfaces of group B1 after a 3-s FCP test, at room temperature, 650 °C and at 704 °C. It is evident that the fracture mode of group B1 is intergranular with well-defined fatigue striations at the temperatures up to 650 °C. It is also interesting to find the deformation pattern of twins. As seen in Fig. 7(c), the slip bands in the matrix could not pass through the twins, they stop at the twin boundary. At the same time, the fracture surface of the twin shows clear river-like cleavage patterns, which indicates that there is another different slip system operating than the one in the matrix. It also can be found that the slip bands in the matrix lead to several micro-cracks in the twin. Fig. 7(d) indicates that the fracture mode of B1 at 704 °C is fully intergranular.

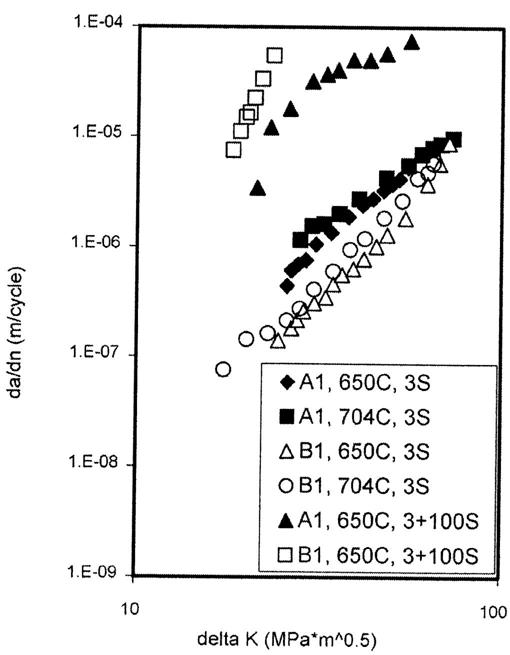

Fig. 5. Fatigue crack propagation rates of A1 and B1.

3.3. FCP of DA alloy

Fig. 8 shows the fatigue crack propagation of the DA 718Plus alloy, as compared to the alloy after conventional heat treatment. It is indicated that the DA sample has slower fatigue crack growth rate than that of the alloy after conventional heat treatment under the 650 °C, 3S condition. Under the 3 + 100S hold-time fatigue condition, the DA and the conventional alloys have almost the same FCP rates.

SEM fractographical analysis (Fig. 9) shows that the alloy obtained elongated grain structure after the DA treatment, as expected. The fracture mode of the DA alloy after 650 °C/3S test is a combination of intergranular and transgranular modes, while the alloy after 650 °C/3 + 100S test shows a predominantly intergranular failure.

The fatigue crack resistances of the DA superalloys are generally different from their conventional counterparts. As proposed by Lynch, etc. [11], the possible differences in microstructure between the DA 718 alloy and the conventional 718 alloy, which could be responsible for the cracking resistance include: (1) the volume fraction, morphology and distribution of carbides and δ-phases; and (2) the grain size, shape, morphology, and grain-boundary-misorientation distributions; rate of grain-boundary diffusion, extent of grain-boundary sliding, and degree by, which the crack branching could be affected. Since most of the microstructural features are interrelated, hence it is difficult to establish their relative importance for the alloys' cracking resistance.

3.4. Long-term exposure effect on FCP

The microstructure of most of Ni-based superalloys will be change after long-term service at high temperatures. In general, there are three major changes in the alloys: (1) grain growth; (2) coarsening of strengthening phases; (3) the transformation of meta-stable phase to equilibrium phase, for instance, gamma double-prime (DO22) to δ-phase transformation. In accordance to the microstructural evolution, the mechanical properties will be changed. Typically, the alloys will lose part of their strength and ductility after long-term exposure.

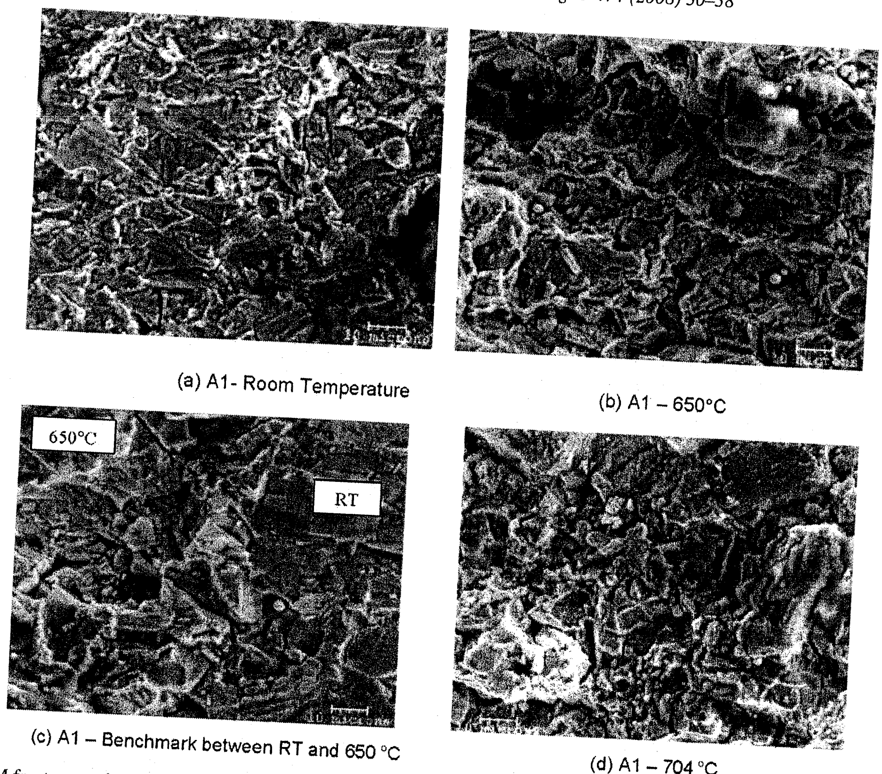

Fig. 6. SEM fracture surface micrograph of A1 after FCG tests with the frequency of 0.33 Hz at room temperature, 650 and 704 °C.

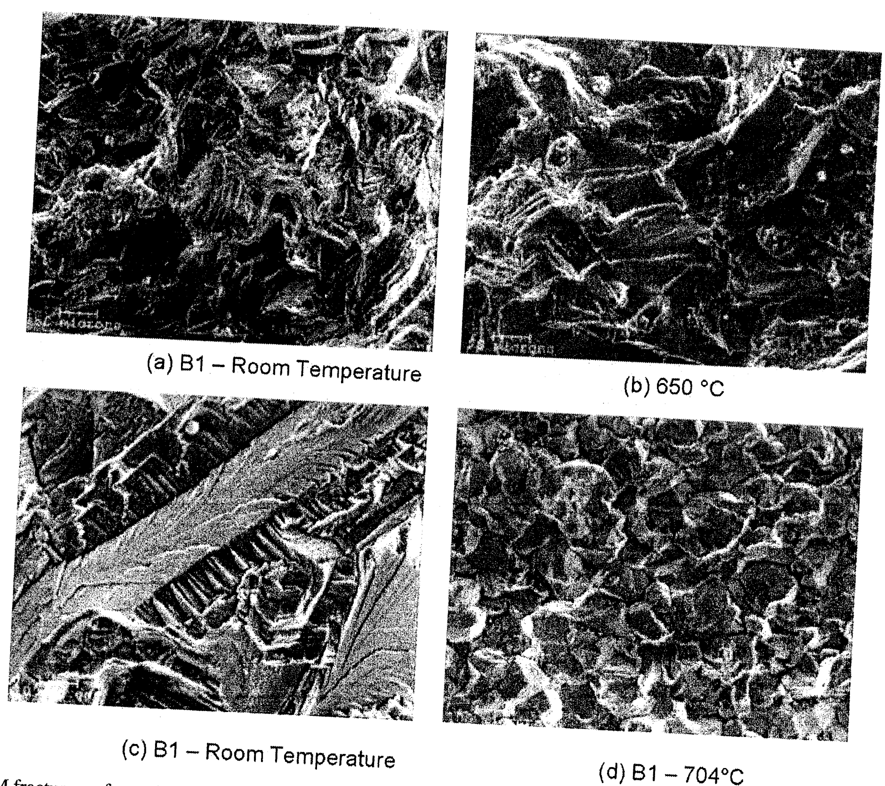

Fig. 7. SEM fracture surface micrograph of B1 after FCG tests with the frequency of 0.33 Hz at room temperature, 650 and 704 °C.

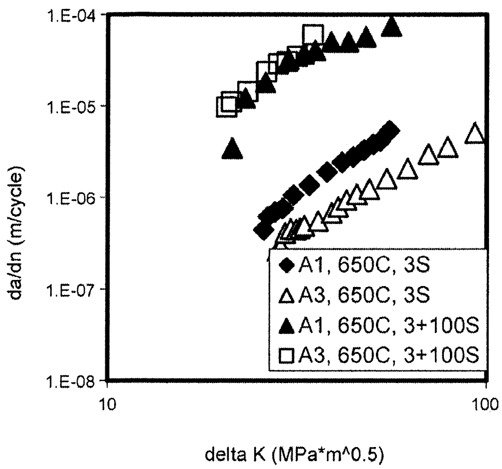

Fig. 8. FCP of DA 718Plus, as compared to the alloy after conventional heat treatment.

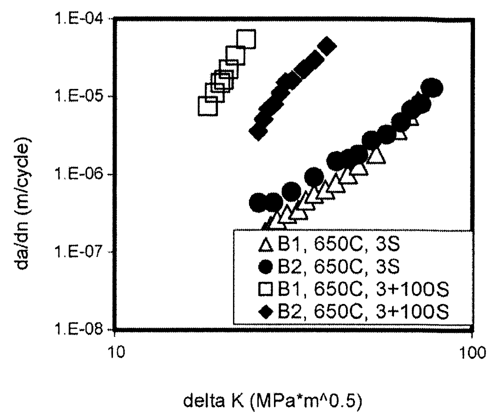

Fig. 10. FCP of the alloy after exposure at 760 °C for 350 h, as compared to the alloy after conventional heat treatment.

In this investigation, the thermal-stability of alloy 718Plus was studied by exposing the alloy at 760 °C for 350 h. Fig. 10 shows the alloy's FCP, as compared to the alloy after conventional heat treatment. It can be seen in the figure that long-term exposure does not change the fatigue crack resistance under 650 °C/3S condition. On the other hand, the hold-time fatigue crack resistance of the alloy was improved by the long-term exposure, which means that this alloy has good long-term structural stability. The reason for this phenomenon needs to be further investigated.

4. Discussions

4.1. Hold-time FCP and grain size effect

Fatigue crack propagation is generally attributed to the damage in front of the crack tip. In the cycle dependent "pure" fatigue, the material in front of the crack tip is damaged only by cyclic loading. However, if the test is conducted at higher temperature and there is a hold-time at max load in the fatigue cycle, the time-dependent behavior must be taken into account. Damage by cyclic loading often produces a smaller amount of the total damage to the materials. Considering the hold-time fatigue, during the hold-time at maximum loading, the material in front of the crack tip is damaged by the diffusion of oxygen and creep, and the resistance against cracking is lowered. During the next unloading and loading, the crack will pass through the damage zone and result in further crack growth. The cycle then repeats again. This kind of crack growth is obviously time-dependent. The size of damage zone represents the resistance of the material against the crack growth. It should be pointed out that the existence of a *damage zone* in several Ni-based superalloys has been confirmed by a specially designed testing method and the damage zone size can be used to evaluate the superalloys' resistance to hold-time FCP [12].

Creep and grain boundary oxygen diffusion/oxidation are the two primary reasons for time-dependent FCP of superalloys, and both are closely related to the grain size and the grain boundary morphology of the alloys. It is generally agreed that coarse-grain alloys should have better resistance to time-dependent FCP than fine-grain alloys, although grain size has little effect on cycle-dependent FCP. For instance, Yuen's study [13] shows that by coarsening the grain size from 22 to 91 μm in alloy 718, near the threshold crack growth rates were reduced and the ΔK_{th} (threshold stress intensity range) values increased. Roughness-

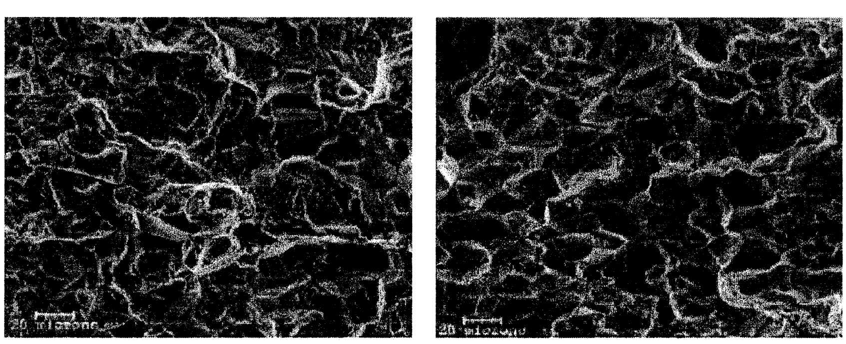

(a) A3, 650°C, 3S (b) A3- 650°C, 3+100S

Fig. 9. SEM fracture surface micrograph of A3 (DA) after FCP tests.

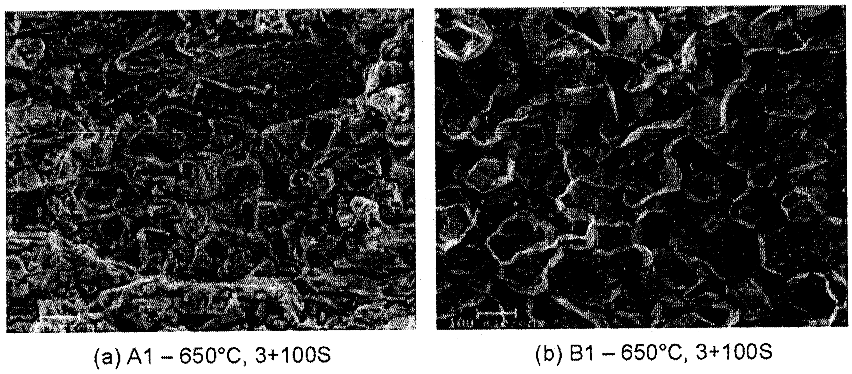

Fig. 11. SEM fracture surface micrograph of A1 and B1 after tested at 650 °C, 3 + 100S.

induced crack closure explains the influence of grain size. The coarse-grain material resulted in much rougher fracture surfaces near threshold growth rates. From grain boundary oxygen diffusion/oxidation point of view, increasing grain size can reduce the total area of the grain boundaries, and therefore, reduce the time-dependent fatigue crack propagation rates of Ni-based superalloys.

The results of this investigation show that on the contrary to those considerations, fine-grain 718Plus alloy (B1) has better resistance to time-dependent FCP, which cannot be explained by above-mentioned mechanisms. Further investigation indicates that the forging route to achieve the coarse-grain also reduces the grain boundary δ-phase precipitation, and this caused the reduction of the alloy's hold-time FCP resistance.

4.2. δ-Phase effect

Since both the δ-phase and the gamma double-prime contain Nb, in the early days the δ-phase was considered as the "detrimental" phase in superalloys because the precipitation of the δ-phase may reduce the alloys' strength by consuming Nb. However, recent investigations show that globular δ-phase distribution along the grain boundaries has a retardation effect on grain boundary crack propagation at the creep/fatigue interaction condition and the existence of reasonable amount of δ-phase can improve stress rupture ductility of the alloy 718 [14]. In addition, the δ-phase has been used to reduce the growth rate of grain size by pinning the grain boundaries. The grain size of the δ-processed (DP) alloy 718 was ASTM 11. As the results indicate, the mechanical properties of the DP 718 alloy were shown to be better than the conventionally processed In718 and the Super Waspaloy at low temperatures [15]. From the environmental effects point of view, the δ-phase in the alloy 718 was found to decrease the environmental effects due to its intrinsic oxidation resistance, by trapping oxygen at the δ-matrix interfaces, or by depleting the Nb in the matrix so that fewer NbC particles are present [16].

The beneficial effect of the δ-phase on the FCP resistance of the 718Plus alloy was revealed by this investigation. Fig. 11 shows the fractographs of A1 (ASTM 8–10) and B1 (ASTM 4–6) after fatigue testing at 650 °C, 3 + 100S conditions. It is indicated that both samples show intergranular failure under this testing condition. However, further investigation on these micrographs revealed that there were numerous δ-phases precipitated along the grain boundaries of A1 sample, while the grain boundaries of B1 are "clean" with very few δ-phase. As mentioned in the above section, grain size effect cannot explain the difference of hold-time FCPRs between A1 and B1. Therefore, the better resistance of B1 to hold-time FCP can be attributed to the grain boundary precipitation of the δ-phase.

To confirm the above discussion on the δ-phase effect and to improve the alloy's hold-time FCP resistance by the optimization of the δ-phase distribution, a pre-solution treatment (PST) at 857 °C for up to 24 h was added before the conventional heat treatment of the alloy. Fig. 12 shows the PST alloy's FCP, as compared to that of the conventional alloy. It can be seen in the figure that the steady state (stage II) FCP of PST alloy are the same as that of the conventional alloy under 650 °C, 3S condition. However, pre-treatment does improve the hold-time FCP resistance of the alloy under 650 °C, 3 + 100S condition. Although the PST alloy has the same crack growth rate when ΔK is close to ΔK_{th}, the slope of the crack growth curve for the PST alloy is much lower than that of the conventional alloy. The other effect of the pre-treatment is the offset of stage III FCG under 650 °C/3S condition. Stage III FCG of the alloy with pre-

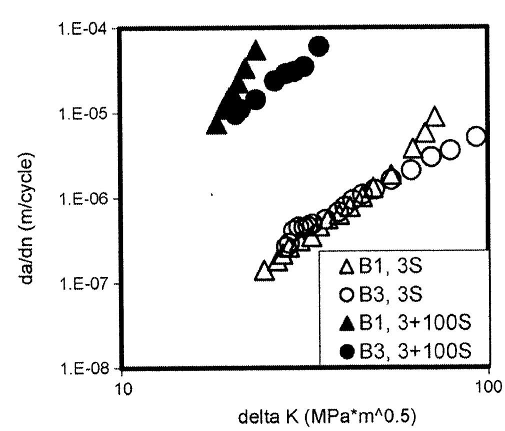

Fig. 12. FCP of the alloy with pre-solution treatment at 857 °C, as compared to the conventional alloy.

treatment appears later than that of the conventional alloy, which results in longer fatigue crack life of the alloy.

4.3. Other issues

The alloys' microstructural characteristics have strong effects on the mechanical properties such as yield strength, creep, and stress relaxation, and could affect crack growth rates. During the time-dependent fatigue crack tests, both creep and environmental degradation can happen during the hold-time. Since both creep and environmental degradation are related to grain boundary behavior, increasing grain size can generally improve the resistance of the alloys to time-dependent FCP by reducing the total surface area of grain boundaries. Regarding strengthening precipitates, decreasing the γ' size from 100 to 10 nm in Waspaloy is observed to increase the FCP resistance by an approximate factor of 3 [3]. The investigation [17] of Waspaloy revealed that the fatigue crack resistance can be improved by increasing the volume fraction of γ' strengthening precipitates. The crack growth rates of the alloy at 650 °C were time-dependent, as expected. However, a higher precipitate content showed a lower time dependency. It was explained that γ' precipitation can increase the grain boundary segregation of Cr, since the Cr solubility is very low in γ' phase. Our research results on Inconel 718 by means of Auger analyses have confirmed such a Cr-enrichment phenomenon [18]. The other effect is that γ' precipitates along the grain boundaries can act as a barrier to the crack growth and deflect the crack growth path during FCP [17].

Besides the strengthening phases γ' and γ'', other grain boundary phases can play a significant role in LCF and hold-time FCP of the superalloys. For instance, several detrimental phases, including G-phase, σ-phase, and Laves phase, can embrittle the superalloys; on the other hand, grain boundary δ-phase has been proved to improve the FCP of the Inconel 718 alloy [4]. The investigation on the Inconel 783 alloy revealed that the grain boundary β-phase improves the hold-time FCP resistance of the alloy by improving the alloys' environmental degradation resistance, deflecting crack path, and oxide-induced crack closure [5,6].

5. Summary and conclusions

The effect of various thermal treatments, including direct aging, pre-solution treatment, and long-term exposure, on the hold-time fatigue crack propagation behavior of the 718Plus alloy were studied and several conclusions can be drawn from this investigation:

1. The alloy shows elongated grain structure after direct aging. The hold-time fatigue crack growth rates of the DA sample are almost the same as that of the alloy after conventional solution plus age treatment.
2. The long-term exposure tests showed that the alloy's hold-time fatigue crack resistance was improved after being exposed at 760 °C for 350 h, which means that this alloy has good long-term structural stability.
3. The fine-grain alloy shows better hold-time FCP resistance than coarse-grain alloy, which is most likely attributed to the δ-phase effect.
4. The result shows that after pre-solution treatment at 857 °C, the alloy's fatigue crack resistance is improved because of the δ-phase at the grain boundaries. The optimum distribution of the δ-phase at the grain boundary needs to be determined in future studies.

Acknowledgements

This research was supported by ATI Allvac (Monroe, NC, USA) and Reference Metals Co. (Bridgeville, PA, USA). The authors would like to thank Mr. Tadeu Carneiro from Companhia Brasileira de Metalurgia e Mineração for his financial support and technical contributions to this research. We also thank Rajeev Dastane for reading the manuscript before submission.

References

[1] L. Garimella, P. Liaw, D. Klarstrom, JOM 49 (1997) 67.
[2] M. Cao, F. Gabrielli, R. Pelloux, Res. Mech. 17 (1986) 163.
[3] S.D. Antolovich, N. Jayaraman, Fatigue: Environment and Temperature Effects, 1983, p. 119.
[4] S. Li, et al., Superalloys 718, 625, 706 and Various Derivatives, TMS, 1994, p. 545.
[5] L. Ma, K.-M. Chang, Scripta Mater. 48 (2003) 583.
[6] L. Ma, K.-M. Chang, Scripta Mater. 48 (2003) 557.
[7] W.D. Cao, R. Kennedy, in: K.A. Green, et al. (Eds.), Superalloys 2004, TMS, 2004, p. 91.
[8] R.L. Kennedy, et al., in: Y.W. Kim, et al. (Eds.), Niobium, High Temperature Applications, TMS, 2003, p. 11.
[9] W.D. Cao, R.L. Kennedy, Acta Metall. Sinica 18 (2005) 39.
[10] X. Liu, et al., in: K.A. Green, et al. (Eds.), Superalloys 2004, TMS, 2004, p. 283.
[11] S.P. Lynch, et al., Fatigue Fract. Eng. Mater. Struct. 17 (1994) 313.
[12] X. Liu, K.-M. Chang, in: E. Loria (Ed.), Superalloys 718, 625, 706 and Various Derivatives, TMS, 2001, p. 543.
[13] J.L. Yuen, P. Roy, Scripta Metall. 19 (1985) 17–22.
[14] S. Li, et al., in: E. Loria (Ed.), Superalloys 718, 625, 706 and Various Derivatives, TMS, 1994, p. 545.
[15] C. Ruiz, A. Obabueki, K. Gillespie, in: S.D. Antolovich, et al. (Eds.), Superalloys 1992, TMS, 1992, p. 33.
[16] S.P. Antolovich, in: E. Loria (Ed.), Superalloys 718—Metallurgy and Applications, TMS, 1989, p. 647.
[17] K.-M. Chang, X. Liu, Mater. Sci. Eng. A A308 (2001) 1.
[18] J. Dong, X. Liu, Acta Metall. Sinica (Engl. Lett.) 10 (1997) 510.